

## 盐酸昌欣沙星抑制开放状态的 HERG 钾通道

张香梅<sup>1</sup>, 朱中华<sup>1</sup>, 孙晓莉<sup>1</sup>, 郭 佳<sup>1</sup>, 赵钟钟<sup>1,2</sup>, 张 朝<sup>1,2\*</sup>

(南京师范大学生命科学学院 1. 江苏省分子医学生物技术重点实验室, 2. 江苏省超分子医用材料及应用重点实验室, 江苏 南京 210046)

**摘要:** 探讨一种新型氟喹诺酮类抗菌剂盐酸昌欣沙星 (chinoxacin hydrochloride, CFX) 对 HERG (human ether-à-go-go-related gene) 钾离子通道动力学的影响。利用全细胞膜片钳技术, 在 HEK293 细胞中记录异源表达的 HERG 钾电流, 观察 CFX 对通道的抑制作用, 分析其对通道激活、失活和去激活等动力学过程的影响。结果表明, CFX 作用于 HERG 钾离子通道的开放状态, 以浓度依赖的方式抑制 HERG 钾电流, 半有效抑制浓度 ( $IC_{50}$ ) 为  $(162.1 \pm 14.2) \mu\text{mol} \cdot \text{L}^{-1}$ , 是其改造前体盐酸莫西沙星的 2 倍, 但 CFX 不改变通道动力学特性。由于改变细胞外液  $K^+$  浓度, CFX 对 HERG 钾电流抑制作用增强。

**关键词:** 盐酸昌欣沙星; HERG 钾离子通道; 氟喹诺酮

中图分类号: R966; R978.69

文献标识码: A

文章编号: 0513-4870 (2010) 12-1491-06

## Chinoxacin hydrochloride inhibits HERG potassium channel at open state

ZHANG Xiang-mei<sup>1</sup>, ZHU Zhong-hua<sup>1</sup>, SUN Xiao-li<sup>1</sup>, GUO Jia<sup>1</sup>, ZHAO Zhong-zhong<sup>1,2</sup>, ZHANG Zhao<sup>1,2\*</sup>

(1. Jiangsu Key Laboratory for Molecular and Medical Biotechnology, 2. Jiangsu Key Laboratory for Supramolecular Medicinal Materials & Applications, College of Life Science, Nanjing Normal University, Nanjing 210046, China)

**Abstract:** This study is designed to investigate the effects of chinoxacin hydrochloride (CFX) on the kinetics of HERG  $K^+$  channel. Whole cell patch clamp technique was used to record HERG  $K^+$  currents from HEK293 cells transiently transfected with cgi-HERG-GFP plasmids and channel kinetics were assessed in the absence and presence of CFX and moxifloxacin hydrochloride (MOX). Results demonstrated that the open state of HERG  $K^+$  channel was inhibited by CFX in a concentration- and time-dependent manner, with an  $IC_{50}$  of  $162.1 \pm 14.2 \mu\text{mol} \cdot \text{L}^{-1}$ , two folds higher than its positive control MOX. But there were no significant effects on channel kinetics. In addition, the inhibitory effect of CFX on HERG was enhanced when cells were subjected to altered extracellular  $K^+$  concentration.

**Key words:** chinoxacin hydrochloride; HERG potassium channel; fluoroquinolone

HERG (human ether-à-go-go-related gene) 编码心肌延迟整流钾电流快速成分  $I_{Kr}$  (rapid component of delayed rectifier potassium channel) 的  $\alpha$  亚基。 $I_{Kr}$  是心肌动作电位复极化 3 期重要的离子流, 任何原因引起其减少将使心室复极化时程显著延长, 可导致室性心律失常, 甚至尖端扭转性室性心动过速 (TdP),

以体表心电图 QT 间期延长、心源性晕厥和猝死为典型临床特征<sup>[1]</sup>。HERG 突变所致的  $I_{Kr}$  减小以致心肌复极化时程显著延长, 是临床上 2 型长 QT 综合征 (long QT syndromes, LQTS) 发生的分子遗传学基础。而某些药物选择性地阻断心肌  $I_{Kr}$ , 是获得性 LQTS 最常见的原因<sup>[2]</sup>。其中包括 III 类抗心律失常药物以及非心血管药物, 如抗疟药、抗生素和抗菌剂、抗组胺类药物、抗精神病类药物等<sup>[3, 4]</sup>。盐酸昌欣沙星 (CFX) 是新研发的氟喹诺酮类抗菌剂, 尚不清楚其对 HERG 钾离子通道的作用。本研究采用全细胞膜

收稿日期: 2010-07-13.

基金项目: 国家自然科学基金资助项目 (30570662, 30871228).

\*通讯作者 Tel: 86-25-85891915, Fax: 86-25-85891353,

E-mail: zhangzhao@njnu.edu.cn

片钳技术, 考察 CFX 对体外表达 HERG 钾离子通道的影响, 以盐酸莫西沙星 (moxifloxacin hydrochloride, MOX) 为阳性对照, 比较分析 CFX 对通道抑制作用的强度及其对通道动力学的影响, 为临床安全用药提供实验依据。

## 材料与方法

**细胞培养** HEK293 细胞 (购自中国科学院细胞库), 在含 10% 胎牛血清、100  $\mu\text{mL}^{-1}$  青霉素和 100  $\mu\text{g}\cdot\text{mL}^{-1}$  链霉素的 DMEM 中, 置 37  $^{\circ}\text{C}$ 、5%  $\text{CO}_2$  培养箱中培养。用于转染的细胞以 50%~60% 密度种于直径为 15 mm 的盖玻片上, 置培养皿中培养, 次日进行转染, 用磷酸钙法瞬时转染质粒 cgi-GFP-HERG (1  $\mu\text{g}$ ), 转染 48 h 后用于电流记录。

**全细胞膜片钳电流的记录** 所有实验均在 (22  $\pm$  2)  $^{\circ}\text{C}$  进行。取转染 48 h 后的细胞, 用细胞外液持续恒速 (2  $\text{mL}\cdot\text{min}^{-1}$ ) 灌流。于倒置荧光显微镜 (Olympus IX71, 日本) 下寻找边缘清晰独立、发绿色荧光的细胞, 用“全细胞”模式记录其表达的 HERG 钾电流。电压钳制脉冲和电流信号的采集及存储由 pClamp10.0 软件控制。电流信号输入膜片钳放大器 (Axon200B, Molecular Devices, USA), 经数模转换器 (DigiData1440A, Molecular Devices, USA) 转换后储存于计算机。记录加药前 HERG 电流 ( $I_{\text{step}}$  和  $I_{\text{tail}}$ ) 作为对照, 然后换以含不同浓度 CFX 的细胞外液持续灌流 5 min (浓度分别为 1、10、100、1 000 及 10 000  $\mu\text{mol}\cdot\text{L}^{-1}$ ), 分别记录加药后的  $I_{\text{step}}$  和  $I_{\text{tail}}$ 。以所记录电流值除以该细胞膜电容得到电流密度 ( $\text{pA/pF}$ )。

将尾电流标准化处理后, 用 Boltzmann 方程拟合:  $I/I_{\text{max}} = 1/[1 + \exp((V_{1/2} - V_m)/k)]$ , 式中  $V_{1/2}$  为通道达 1/2 激活时的膜电位;  $k$  是斜率因子。计算抑制率: 抑制率 =  $1 - (I_{\text{HERG-CFX}} - I_{\text{HERG-CTL}})/I_{\text{HERG-CTL}}$ ,  $I_{\text{HERG-CTL}}$  和  $I_{\text{HERG-CFX}}$  分别表示加药前后记录的电流 (CTL: Control)。以药物作用浓度为横坐标, 加药后电流抑制的百分比为纵坐标绘制浓度-反应曲线, 经 Logistic 方程拟合得到其半有效抑制浓度 ( $\text{IC}_{50}$ )。

**液体与药品配制** 所用正常细胞外液成分为 ( $\text{mmol}\cdot\text{L}^{-1}$ ): NaCl 140, KCl 5.4,  $\text{MgCl}_2$  1.0,  $\text{CaCl}_2$  1.0, HEPES 10.0, 葡萄糖 10.0, 用 NaOH 调节 pH 至 7.4。为了检测外液钾离子浓度变化时, CFX 对通道的影响是否有变化, 将正常细胞外液中 KCl 降低至 2  $\text{mmol}\cdot\text{L}^{-1}$  或升高至 10  $\text{mmol}\cdot\text{L}^{-1}$ , 则为低钾或高钾液, 其余成分相同, 渗透压用 NaCl 来调整。所用电极内液成分为 ( $\text{mmol}\cdot\text{L}^{-1}$ ): KCl 140.0,  $\text{MgCl}_2$  1.0, HEPES

10.0, EGTA 5.0, K-ATP 4.0, 以 KOH 调节 pH 至 7.3。

CFX (批号: 080402) 与其阳性对照 MOX (批号: BXF6U5B) 由浙江医药股份有限公司提供。用 DMSO 溶至 100  $\text{mmol}\cdot\text{L}^{-1}$  的母液, 于 -20  $^{\circ}\text{C}$  保存, 实验时用细胞外液稀释至工作浓度。

**统计学处理** 所有数据均采用  $\bar{x} \pm s$  表示, 用 pCLAMP10.0 (Molecular Devices, USA) 结合 SPSS10.0 软件分析处理, 以 Origin 6.0 for Windows 作图。同一组或不同组细胞用药前后的比较采用配对  $t$  检验或两样本间均数比较的  $t$  检验; 多组之间比较采用单因素方差分析 (ANOVA) 和  $q$  检验进行统计学处理。

## 结果

### 1 CFX 对 HERG 钾电流的影响

CFX (图 1A) 是由 MOX 的结构改造而来的。一连串脉冲刺激细胞可以记录到典型的 HERG 钾电流 (图 1B), 即将膜电位钳制在 -80 mV, 给予细胞持续 2 s、从 -70 mV 到 +60 mV 以 10 mV 递增的脉冲刺激, 再使细胞膜复极化至 -40 mV, 持续 4 s, 产生尾电流。为了解药物作用的开始时间, 选择能引起最大电流的刺激脉冲<sup>[5]</sup> (钳制电压为 -80 mV, 给予 +20 mV 的刺激, 持续 2 s, 再复极化至 -40 mV, 持续 4 s) 作用于细胞 (图 1C), 用 1 000  $\mu\text{mol}\cdot\text{L}^{-1}$  CFX 灌流细胞时, 1 min 后显示出药物对通道的抑制作用, 5 min 后抑制作用达到最大, 并不再随时间的延长而增强。故后续所有加药后的记录, 均在药物作用 5 min 以后进行。该药物作用可以被完全洗脱, 提示其与通道系可逆结合。为了排除药物溶解介质对 HERG 钾电流的影响, 将溶解 1 000  $\mu\text{mol}\cdot\text{L}^{-1}$  药物同体积的 DMSO 加入灌流液后, 所记录的 HERG 钾电流几乎没有变化。上述不同条件下 (图 1C) 所记录尾电流的统计结果见图 1D。对应于 -70~+60 mV 脉冲刺激 (图 1B), CFX 作用前后阶跃电流和尾电流的比较 (图 1E 和 1F) 显示, CFX 的抑制作用从 -30 mV 开始出现, 随膜电位去极化发展而抑制逐渐增强。就尾电流而言, 在 -40~+20 mV 电压范围内, 药物抑制作用随着去极化电压正向变化而增加, 在 +20 mV 时抑制达峰值, 其后抑制作用饱和。

### 2 CFX 对 HERG 钾电流的浓度依赖性抑制

对同一个细胞以 10、100、1 000  $\mu\text{mol}\cdot\text{L}^{-1}$  累加给药条件下, 从 CFX 对最大电流抑制的情况 (图 2A) 可以看出, CFX 以电压和浓度依赖的方式对 HERG 钾电流产生抑制作用。以药物作用浓度为横坐标、药物抑制电流的百分比为纵坐标, 经 Logistic 方程拟合得

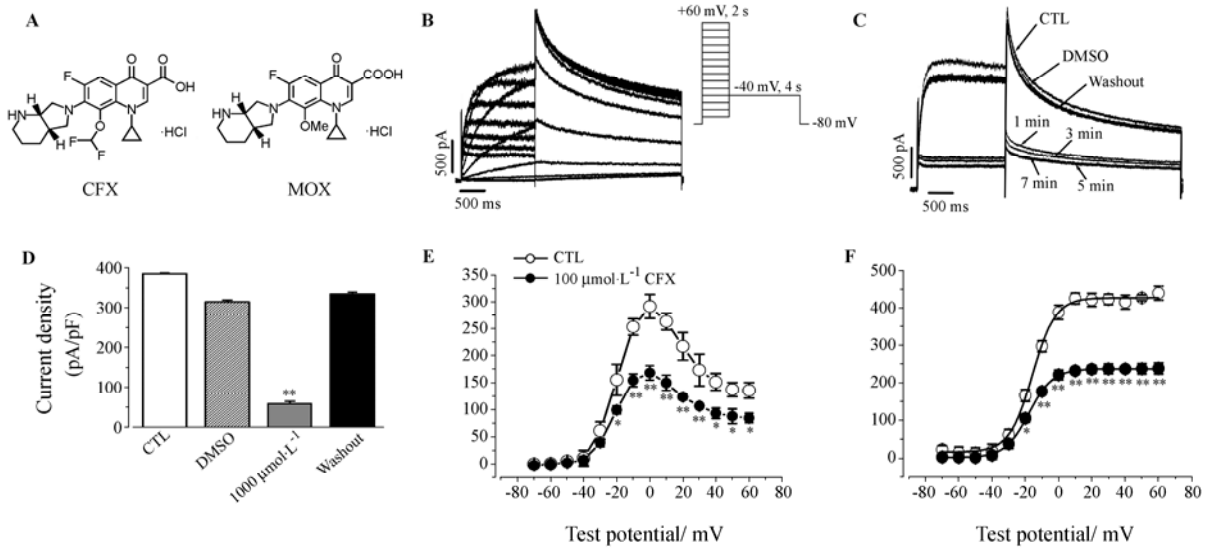


**Figure 1** Inhibitory effects of cinoxacin hydrochloride (CFX) on HERG K<sup>+</sup> currents. A: Chemical structures of CFX reconstructed from moxifloxacin hydrochloride (MOX) and MOX; B: Representative traces of HERG K<sup>+</sup> currents recorded from HEK293 cell transiently transfected with cgi-HERG-GFP using a family of depolarizing pulse protocol shown in inset from holding potential of -80 mV; C: To assess the onset of inhibitory effects, in the same cell as in panel B, the peak current in response to a depolarizing pulse of +20 mV for 2 s was recorded after 1 000  $\mu\text{mol}\cdot\text{L}^{-1}$  CFX exposure for 1, 3, 5, and 7 min. DMSO was used as vehicle control; D: The summarized density of tail currents after DMSO or 1 000  $\mu\text{mol}\cdot\text{L}^{-1}$  drug exposure and washout after exposure to 1 000  $\mu\text{mol}\cdot\text{L}^{-1}$  CFX ( $n = 4$  for each); E and F: Summary of current density-voltage relationship for step and tail currents from control values compared with 100  $\mu\text{mol}\cdot\text{L}^{-1}$  CFX application (\* $P < 0.05$ , \*\* $P < 0.01$  vs CTL). CTL: Control

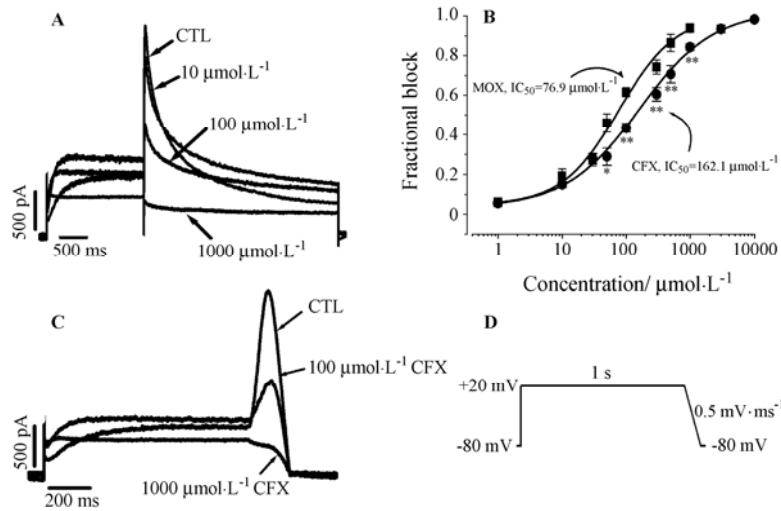


**Figure 2** Concentration-dependence of HERG inhibition by CFX. A: Effects of cumulative concentrations of CFX (10, 100, and 1 000  $\mu\text{mol}\cdot\text{L}^{-1}$ ) on the peak current amplitude elicited by a 2 s depolarizing pulse of +20 mV from holding potential of -80 mV, followed by a 4 s repolarizing pulse of -40 mV; B: A CFX concentration-response curve was generated by fitting data to a Logistic equation of the form  $y = A2 + (A1 - A2)/(1 + (x/x_0)^k)$  ( $n = 7$ ), where A1 and A2 mean the maximal and minimal inhibition,  $x$  refers to the working concentration of drug,  $x_0$  is the IC<sub>50</sub> at which drugs produce a half-maximal inhibition of the HERG K<sup>+</sup> currents. And  $k$  is the slope factor for the fit (\* $P < 0.05$ , \*\* $P < 0.01$  vs MOX); C: Concentration-dependent HERG inhibition induced by CFX was further evidenced by “step-ramp” voltage command as shown in D. Cells were voltage-clamped at -80 mV and depolarized to +20 mV for 1 s followed by a repolarizing ramp back to -80 mV at a rate of 0.5  $\text{mV}\cdot\text{ms}^{-1}$ . The command was applied every 4 s

到浓度-反应曲线 (图 2B), 结果显示 CFX 对 HERG 钾电流的半有效抑制浓度 (IC<sub>50</sub>) 为 (162.1 ± 14.2)  $\mu\text{mol}\cdot\text{L}^{-1}$ , 是其阳性对照 MOX (IC<sub>50</sub> = 76.9 ± 10.2  $\mu\text{mol}\cdot\text{L}^{-1}$ ) 的 2 倍。为了进一步证实这一浓度依赖的

抑制作用, 用 step-ramp 这个模拟动作电位的脉冲刺激<sup>[5]</sup>, 即将膜电位钳制在 -80 mV, 使细胞膜去极化至 +20 mV, 持续 1 s, 再以 0.5  $\text{mV}\cdot\text{ms}^{-1}$  复极化至 -80 mV, 比较加药前后记录的电流, 可见药物抑制作用

同样有浓度依赖性 (图 2C)。

### 3 CFX 对 HERG 钾通道动力学的影响和时间依赖性的抑制作用

$100 \mu\text{mol}\cdot\text{L}^{-1}$  CFX 作用对通道门控动力学影响的结果见图 3A、C 和 E。分析数据显示, CFX 使通道的稳态激活曲线左移约  $4.3 \text{ mV}$  (图 3B), 但与对照相比差异无显著性。对稳态失活 (图 3D)、去激活 (图 3F) 和从失活状态恢复的时间常数  $\tau$  值则无显著影响 (数据未显示)。提示 CFX 结合于通道的开放状态。

为了解 CFX 抑制 HERG 钾通道的时间依赖性, 选用两种不同的脉冲刺激方式记录电流。首先, 用经典的 Envelop 模式观察 CFX 对 HERG 钾电流的抑制作用。如图 4A 所示, 将膜电位维持在  $-80 \text{ mV}$ , 给予细胞  $+20 \text{ mV}$  去极化刺激, 持续时间从  $10 \text{ ms}$  至  $1400 \text{ ms}$ , 以  $100 \text{ ms}$  逐渐增加, 再去极化至  $-40 \text{ mV}$ , 持续  $5 \text{ s}$ 。此法记录到的随刺激持续时间延长而逐渐增大

的尾电流, 可以反映通道激活的时程或速率<sup>[6, 7]</sup>, 并了解药物作用的启动时间<sup>[8]</sup>。以脉冲持续时间为横坐标、所记录的尾电流峰值为纵坐标, 经单指数方程拟合得到图 4B 曲线。用  $100 \mu\text{mol}\cdot\text{L}^{-1}$  CFX 处理前后通道激活时间常数分别为  $(176.3 \pm 9.4)$  和  $(168.9 \pm 2.9) \text{ ms}$ , 提示 CFX 减少通道激活时程, 换言之, 加速了激活速率。此外, 可以看出当去极化时间较短, 通道几乎不开放的时候, 抑制作用很小; 当通道完全开放时 (去极化刺激持续时间约  $500 \text{ ms}$ ), 抑制作用达到最大。其后, 随着时间继续延长, 药物阻断作用达平台期。其次, 用持续时间长达  $10 \text{ s}$ 、去极化到  $+20 \text{ mV}$  的单脉冲刺激方式作用于细胞 (此时通道可能存在开放和失活状态), 记录对照电流后, 在膜电位维持在  $-80 \text{ mV}$  的条件下 (使通道关闭) 加入药物, 待其作用  $10 \text{ min}$  后, 再重复脉冲刺激 (图 4C)。结果如图 4D 所示, 药物抑制作用呈时相性, 即脉冲起始抑制

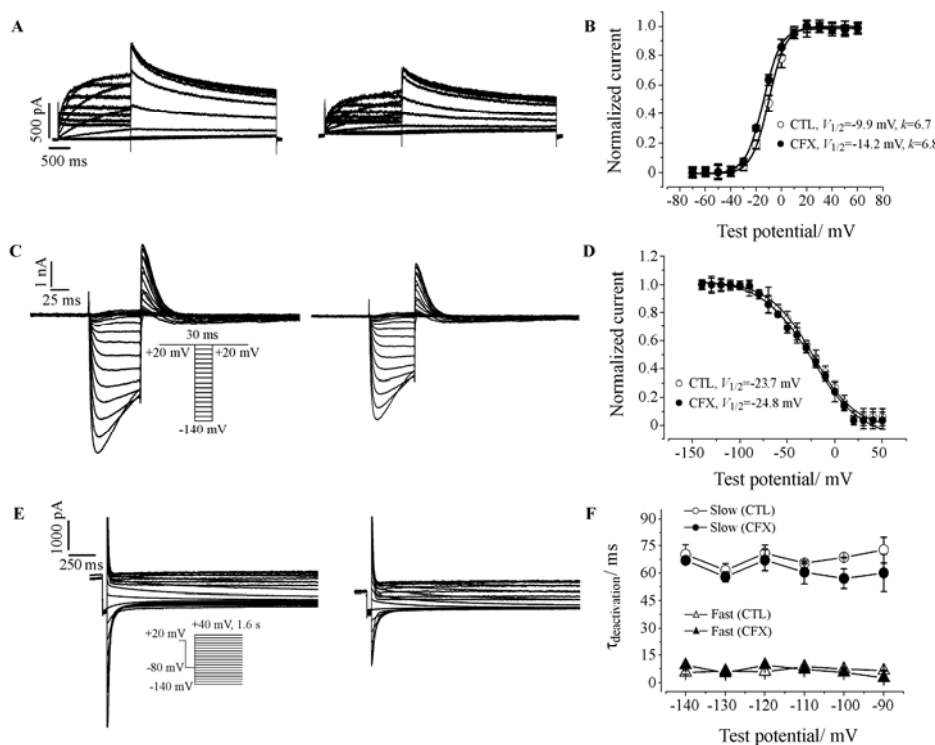


**Figure 3** Effects of CFX on kinetics of HERG K<sup>+</sup> channel. A: HERG K<sup>+</sup> currents recorded in control conditions and with  $100 \mu\text{mol}\cdot\text{L}^{-1}$  CFX. B: Peak tail currents are plotted as a function of the preceding test pulse potential resulting in activation curves (mean data of  $n = 6$  experiments). Data were fitted to the Boltzmann equation (shown in methods). Half-maximal activation voltage  $V_{1/2}$  was  $-9.9 \pm 1.1 \text{ mV}$  ( $k = 6.7$ ) under control conditions and  $-14.2 \pm 0.7 \text{ mV}$  ( $k = 6.8$ ) after application of CFX ( $P > 0.05$ ). C: Example traces in this panel illustrate the effects of CFX on inactivation kinetics. D: Steady-state inactivation was measured with two-pulse protocol (see inset of C), in which a pulse step to  $+20 \text{ mV}$  followed by a successive  $30 \text{ ms}$  test to potentials ranging from  $-140$  to  $+40 \text{ mV}$  in  $10 \text{ mV}$  increments and a second test pulse to  $+20 \text{ mV}$ . The steady-state inactivation curves were illustrated under control (open circle) condition and CFX exposure (filled circle). Outward current amplitudes induced by second step to  $+20 \text{ mV}$  were measured and normalized values were plotted as a function of the preceding test potentials. By fitting the curves with a Boltzmann equation, the mean values of  $V_{1/2}$  inactivation were  $-23.7 \text{ mV}$  ( $k = 22.7$ ) and  $-24.8 \text{ mV}$  ( $k = 25.9$ ) for control and CFX exposure, respectively. No significant shift of the inactivation curve was observed ( $n = 5$ ). E: Example traces in this panel show the effects of CFX on deactivation kinetics. F: The time course for deactivation was examined by fitting the decay of tail current with the double exponential function yielding the fast ( $\tau_{\text{fast}}$ ) and slow ( $\tau_{\text{slow}}$ ) time constants. There were no significant differences in the fast or slow deactivation time constants before and after CFX application ( $n = 7$ ).

作用为 0, 在 500 ms 左右即达到稳态, 并不再随刺激持续时间延长而增加。药物对通道作用进展快速, 在 100 ms 内已达 80%, 进一步提示 CFX 作用于 HERG 通道的开放状态。

#### 4 改变细胞外液钾离子浓度对 CFX 抑制 HERG 钾电流作用的影响

对药物诱导的心律失常患者的基因分析表明, 10%~15% 的患者具有先天的 LQTS 的基因突变, 当患者处于严重心动过缓、心肌缺血、电解质代谢紊乱时, 更容易导致获得性 LQTS<sup>[9]</sup>。为进一步分析胞外钾

离子浓度改变对 CFX 抑制 HERG 钾电流作用的影响, 观察比较了细胞外液中钾离子浓度升高 ( $10 \text{ mmol} \cdot \text{L}^{-1}$ ) 和降低 ( $2 \text{ mmol} \cdot \text{L}^{-1}$ ) 时 CFX 的作用 (图 5)。HERG 通道作为外向的钾离子通道, 其离子驱动力由膜内外电化学势能差决定, 当外液中的钾离子浓度升高时, 钾离子向外的驱动力减少, 因此这种情况即使不加药, 电流也有所减小, 相反当外液中的钾离子浓度降低时, 电流相应增大。但是与  $300 \mu\text{mol} \cdot \text{L}^{-1}$  CFX (正常细胞外液) 单独作用相比, 细胞外液中钾离子浓度无论升高或降低, 药物抑制作用均明显增强。

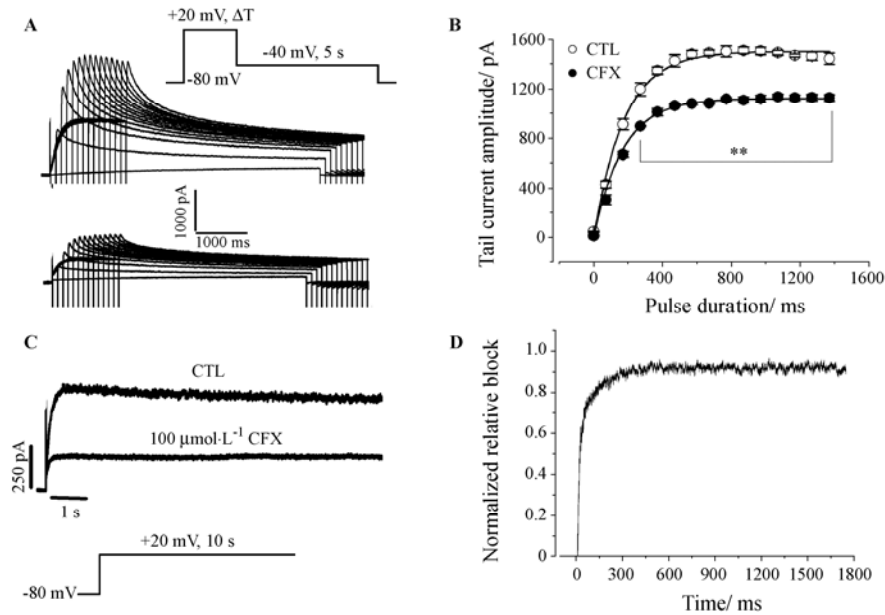


**Figure 4** Time-dependence of HERG inhibition by CFX. A: An Envelope of tails protocol, as illustrated in the inset, was used to evaluate time-dependence of channel inhibition. Cell membrane were depolarized to +20 mV for periods of time from 10 to 1 400 ms before repolarizing to -40 mV to induce tail currents. Peak tail currents were measured at control conditions and after application of  $100 \mu\text{mol} \cdot \text{L}^{-1}$  CFX. B: This panel shows the increase in tail current with length of the depolarizing step for the cell illustrated in (A), in the absence and presence of CFX ( $n = 4$ ,  $**P < 0.01$ ). C: A long duration (10 s) of +20 mV depolarizing pulse from the holding potential of -80 mV (as shown in inset) was applied to the cell and then steady-state response was observed before and after CFX application. Full extent of block was observed within 500 ms and maintained for 10 s duration. D: Normalized relative block is plotted versus time after the voltage step to 0 mV. This gave the CFX-sensitive current which showed phasic development of complete inhibition, a sign for open channel block

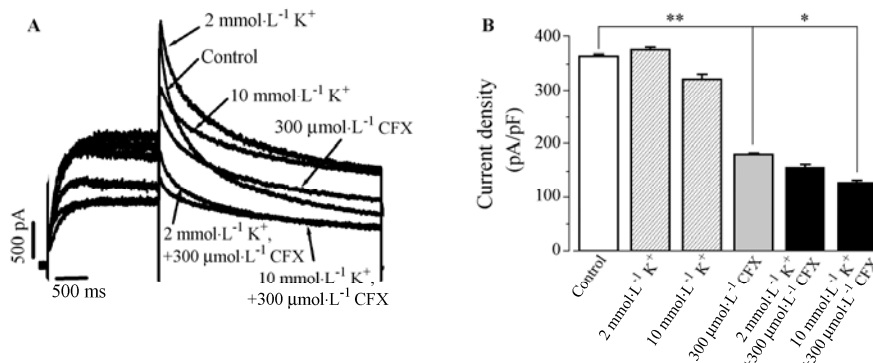


**Figure 5** Effects of extracellular  $\text{K}^+$  concentration on CFX-induced HERG inhibition. A: Superimposed HERG  $\text{K}^+$  currents elicited from cells bathed in extracellular solution containing 2 and  $10 \text{ mmol} \cdot \text{L}^{-1} \text{K}^+$  were compared to those at control condition ( $5.4 \text{ mmol} \cdot \text{L}^{-1} \text{K}^+$ ) in the presence of  $300 \mu\text{mol} \cdot \text{L}^{-1}$  CFX. B: Summarized data for the effects of extracellular  $\text{K}^+$  on CFX-induced HERG inhibition ( $n = 4$ ;  $**P < 0.01$  grey bar vs open bar;  $*P < 0.05$  black bar vs grey bar)

## 讨论

氟喹诺酮类抗菌药是广泛用于感染性疾病的第三代喹诺酮类广谱抗菌剂,对革兰阳性菌、革兰阴性菌、支原体和某些厌氧菌均有效。然而,随着氟喹诺酮类临床应用的增加,某些品种引起LQTS综合征的报道也不断增多,如司帕沙星(sparfloxacin)、加替沙星(gatifloxacin)、格里沙星(grepafloxacin)和MOX等<sup>[5, 10, 11]</sup>。而这些无一例外地与其阻断HERG钾离子通道有关。因此,药物阻断HERG钾离子通道引起心律失常的不良反应,是药物研发过程中必须要考虑的重要问题。CFX是一种新型的氟喹诺酮类抗菌药,由MOX的结构改造而来(将MOX基本结构喹啉环C<sub>8</sub>侧链上的甲基替代为2个氟原子)。这种结构改造是否减弱了其对HERG钾离子通道的抑制作用,是本研究关注的主要内容。实验结果表明,CFX以浓度、时间和电压依赖的方式抑制HERG钾电流,这种抑制作用以在通道开放时为显著。对通道动力学分析的结果显示,CFX不影响通道的稳态激活、稳态失活过程,也不影响其从失活状态恢复的时间,提示药物不影响通道蛋白本身随着膜电位改变而引起空间构象的变化,与其他氟喹诺酮类抗菌药作用相似。但CFX加速通道开放速率,使激活时程缩短,这一点与其改造前体MOX类似<sup>[5]</sup>。CFX阻断作用进展快,与开放状态的通道有较高亲和力,推测是其抑制HERG钾电流的主要机制。CFX对HERG尾电流的半有效抑制浓度为 $(162.1 \pm 14.2) \mu\text{mol}\cdot\text{L}^{-1}$ ,是MOX $(76.9 \pm 10.2 \mu\text{mol}\cdot\text{L}^{-1})$ 的2倍,表明经过改造后的CFX对HERG电流的抑制作用减弱。

动物体内药代动力学研究结果显示(未发表的数据),CFX灌胃给药后在大鼠和比格犬体内吸收迅速,平均血浆达峰时间为0.7和1.2 h,血浆消除半衰期平均为3.4和10.2 h。以 $4.0 \text{ mg}\cdot\text{kg}^{-1}$ 剂量给大鼠灌胃后, $C_{\text{max}}$ 为 $0.4 \text{ mg}\cdot\text{L}^{-1}$  ( $0.9 \mu\text{mol}\cdot\text{L}^{-1}$ );以 $4.5 \text{ mg}\cdot\text{kg}^{-1}$ 剂量给比格犬灌胃,其 $C_{\text{max}}$ 为 $1.8 \text{ mg}\cdot\text{L}^{-1}$  ( $3.8 \mu\text{mol}\cdot\text{L}^{-1}$ ),而本研究得到CFX抑制HERG尾电流的 $\text{IC}_{50}$ 为 $(162.1 \pm 14.2) \mu\text{mol}\cdot\text{L}^{-1}$ ,分别是大鼠 $C_{\text{max}}$ 的179.5倍,犬 $C_{\text{max}}$ 的43.2倍。就动物实验而言,CFX对HERG的抑制作用远大于Redfern等<sup>[12]</sup>提出的 $\text{IC}_{50}/C_{\text{max}} > 30$ 安全极限。

药物引起LQTS的因素很复杂,除了药物作用于通道本身外,女性或患有其他疾病,例如代谢性疾病、电解质紊乱等,均可以增加患者对药物的敏感性,使药物诱发LQTS的可能增加。本实验中也观察到,细胞外液钾离子浓度无论增高或降低,与在正常细胞

外液条件下相比,同一浓度CFX对HERG电流显示更强的抑制作用,其中以钾离子浓度降低更明显。这提示,胞外钾离子浓度可影响通道对药物的敏感性。

综上所述,尽管经过改造后CFX心脏毒性有所减弱,但如果应用于临床,对电解质代谢紊乱或伴有其他疾病的患者,仍应审慎使用。

## References

- [1] Sanguinetti MC, Tristani-Firouzi M. hERG potassium channels and cardiac arrhythmia [J]. *Nature*, 2006, 440: 463–469.
- [2] Sanguinetti MC, Chen J, Fernandez D, et al. Physicochemical basis for binding and voltage-dependent block of hERG channels by structurally diverse drugs [J]. *Novartis Found Symp*, 2005, 266: 159–166; discussion 166–170.
- [3] Mitcheson JS. hERG potassium channels and the structural basis of drug-induced arrhythmias [J]. *Chem Res Toxicol*, 2008, 21: 1005–1010.
- [4] Stansfeld PJ, Gedeck P, Gosling M, et al. Drug block of the hERG potassium channel: insight from modeling [J]. *Proteins*, 2007, 68: 568–580.
- [5] Alexandrou AJ, Duncan RS, Sullivan A, et al. Mechanism of hERG K<sup>+</sup> channel blockade by the fluoroquinolone antibiotic moxifloxacin [J]. *Br J Pharmacol*, 2006, 147: 905–916.
- [6] Su Z, Limberis J, Souers A, et al. Electrophysiologic characterization of a novel hERG channel activator [J]. *Biochem Pharmacol*, 2009, 77: 1383–1390.
- [7] Zhou Z, Gong Q, Ye B, et al. Properties of HERG channels stably expressed in HEK 293 cells studied at physiological temperature [J]. *Biophys J*, 1998, 74: 230–241.
- [8] Zitron E, Karle CA, Wendt-Nordahl G, et al. Bertosamil blocks HERG potassium channels in their open and inactivated states [J]. *Br J Pharmacol*, 2002, 137: 221–228.
- [9] Yang P, Kanki H, Drolet B, et al. Allelic variants in long-QT disease genes in patients with drug-associated torsades de pointes [J]. *Circulation*, 2002, 105: 1943–1948.
- [10] Kang J, Wang L, Chen XL, et al. Interactions of a series of fluoroquinolone antibacterial drugs with the human cardiac K<sup>+</sup> channel HERG [J]. *Mol Pharmacol*, 2001, 59: 122–126.
- [11] Ducrocq J, Moha ou Maati H, Guilbot S, et al. Dexrazoxane protects the heart from acute doxorubicin-induced QT prolongation: a key role for I(Ks) [J]. *Br J Pharmacol*, 2010, 159: 93–101.
- [12] Redfern WS, Carlsson L, Davis AS, et al. Relationships between preclinical cardiac electrophysiology, clinical QT interval prolongation and torsade de pointes for a broad range of drugs: evidence for a provisional safety margin in drug development [J]. *Cardiovasc Res*, 2003, 58: 32–45.

## The transport of gastrodin in Caco-2 cells and uptake in Bcap37 and Bcap37/MDR1 cells

WANG Xiao-dan<sup>1,2</sup>, ZENG Su<sup>2\*</sup>

(1. The Second Hospital of Wuxi, Wuxi 214002, China;

2. College of Pharmaceutical Sciences, Zhejiang University, Hangzhou 310058, China)

**Abstract:** Gastrodin (GAS) is the major bioactive component of the extracts from the rhizome of *Gastrodia elata* Blume. The aim of this study is to investigate the transport of GAS in Caco-2 cells and the interaction of P-glycoprotein and GAS. The apparent permeability coefficients ( $P_{app}$ ) of GAS were measured as a function of directions and concentrations. It was demonstrated that the efflux ratio was  $< 2.0$  over the range of 50–500  $\mu\text{mol}\cdot\text{L}^{-1}$  of GAS from bi-directional transport studies. The transport rate of GAS was dependent on the concentrations.  $P_{app}$  of GAS was not affected by transport directions, GAS concentration or the classical inhibitors of P-glycoprotein (verapamil and GF 120918). The cellular accumulation of GAS in Bcap37/MDR1 cells transfected with hMDR1 gene, was similar to that in Bcap37 cells. The accumulation in both cell lines was concentration dependent. GAS did not affect the accumulation of Rhodamine 123 in Bcap37/MDR1 cells over the range of 50–500  $\mu\text{mol}\cdot\text{L}^{-1}$ . It indicated that the transport of GAS in Caco-2 cell monolayers mainly is by passive paracellular transport pathway. P-glycoprotein did not participate in the absorption of GAS in the intestine or the transport across the blood-brain barrier.

**Key words:** gastrodin; P-glycoprotein; Caco-2 cell; Bcap37 cell

**CLC number:** R965.1

**Document code:** A

**Article ID:** 0513-4870 (2010) 12-1497-06

## 天麻素在 Caco-2 细胞及 Bcap37、Bcap37/MDR1 细胞模型中的转运和摄取

王晓丹<sup>1,2</sup>, 曾 苏<sup>2\*</sup>

(1. 无锡市第二人民医院, 江苏 无锡 214002; 2. 浙江大学药学院, 浙江 杭州 310058)

**摘要:** 天麻素是传统中药天麻的有效活性成分。本研究以 Caco-2 细胞、Bcap37 和 Bcap37/MDR1 为模型, 体外评价天麻素在 Caco-2 细胞模型上的转运过程以及天麻素与 P-糖蛋白之间的相互作用。在 50~500  $\mu\text{mol}\cdot\text{L}^{-1}$  浓度内, 天麻素的表观渗透系数 ( $P_{app}$ ) 比值  $< 2.0$ , 与转运方向无关, 且不受 P-糖蛋白的经典抑制剂 (维拉帕米和 GF120918) 的影响。天麻素在 Bcap37、Bcap37/MDR1 细胞中的积聚呈浓度依赖性, 且干扰罗丹明 123 在 Bcap37/MDR1 细胞中的积聚。结果表明, 天麻素在 Caco-2 细胞模型上的转运方式以被动转运为主, 天麻素不是 P-糖蛋白的底物和抑制剂。

**关键词:** 天麻素; P-糖蛋白; Caco-2 细胞; Bcap37 细胞

Received 2010-08-01.

Project supported by National Key Project of China (2009ZX09304-003).

\*Corresponding author Tel / Fax: 86-571-88208407, E-mail: zengsu@zju.edu.cn